Rev. Int. Contam. Ambie. 39, 307-317, 2023
https://doi.org/10.20937/RICA.54830

INVESTIGATION OF FACTORS AFFECTING REMOVAL OF ARSENIC FROM POLLUTED WATER USING IRON-BASED PARTICLES: TAGUCHI OPTIMIZATION DESIGN

Investigación de los factores que afectan la eliminación de arsénico del agua contaminada utilizando partículas a base de hierro: diseño de optimización de Taguchi

Shafagh MOLAEI[1], Mohsen HAMIDPOUR[1]*, Hossein SHIRANI[1] and Mohammad SABET[2]

[1] Department of Soil Science, College of Agriculture, Vali-e-Asr University of Rafsanjan, P.O. Box 518, Rafsanjan, Iran.
[2] Department of Chemistry, College of Basic Science, Vali-e-Asr University of Rafsanjan, P.O. Box 518, Rafsanjan, Iran.

*Author for correspondence: m.hamidpour@vru.ac.ir

(Received: May 2022; accepted: January 2023)

Key words: adsorption, adsorbents, heavy metals, environmental pollution, isotherms.

ABSTRACT

Intensive research efforts have been followed to remove arsenic (As) from contaminated water to provide potable water to millions living in different countries. Adsorption is a simple and efficient way for arsenic contamination purification in water, with a pressing challenge to find a cheap and efficient adsorbent. The present paper deals with optimizing various batch parameters for the adsorption of As from solution by synthesized iron-based particles (hematite, magnetite, and zero-valent iron (ZVI)) nanomaterials using Taguchi's optimization methodology. Taguchi's (L27) orthogonal design with six effective factors, namely: initial As concentration, pH, contact time, adsorbent type, size, and dose, was applied for the multivariate optimization in adsorption studies for As to maximize the adsorption capacity along with the signal-to-noise ratio. The equilibrium studies revealed that the data were well described by Freundlich isotherm. The results showed that initial As concentration was the most important parameter in the adsorption process.

Palabras clave: adsorción, adsorbentes, metales pesados, contaminación ambiental, isotermas.

RESUMEN

Se han llevado a cabo intensas investigaciones para eliminar el arsénico (As) del agua contaminada a fin de proporcionar agua potable para millones de personas que viven en diferentes países. La adsorción es una forma simple y eficiente para la eliminación del arsénico en el agua, pero hay desafío apremiante para encontrar un adsorbente barato y eficiente. El presente trabajo se ocupa de la optimización de varios parámetros en lote para la adsorción de As en solución por nanomateriales sintetizados a base de hierro (hematita, magnetita y hierro cero valente (ZVI)) utilizando la metodología de optimización de Taguchi. El diseño ortogonal de Taguchi (L27) con seis factores efectivos, a saber: concentración inicial, pH, tiempo de contacto, tipo de adsorbente, tamaño y dosis, se aplicó para la optimización multivariable para maximizar la capacidad de

adsorción junto con la relación señal-ruido. Los estudios de equilibrio revelaron que los datos fueron bien descritos por la isoterma de Freundlich. Los resultados muestran que la concentración de As fue el parámetro más importante en el proceso de adsorción.

INTRODUCTION

There is a great concern about arsenic (As) pollution, which is the foremost harmful and carcinogenic chemical substance and is regarded by the World Health Organization (WHO) as the first priority issue among the toxic compounds (Zhu et al. 2009, Ajiboye et al. 2021). Also, it has been recognized as a group 1 carcinogen by the International Agency for Research on Cancer (Hao et al. 2018).

In recent years, a number of methods have been utilized for the removal of As from contaminated water, including reverse osmosis, electrodialysis, ion exchanges, membrane filtration, precipitation, and adsorption (Chaudhry et al. 2017, Uddin and Jeong 2020). Adsorption has been widely used as a low-cost, high efficiency, simple and sludge-free method for treating heavy metal contamination in water. However, a low-cost and highly efficient As adsorbent is currently needed for the real application of this technique (Hao et al. 2018, Cao et al. 2021). Various materials have been used for the removal of As from polluted water and waste waters. Because of high specific surface area, high adsorption capacity, strong affinity and low cost, iron-based adsorbents (e.g. iron oxide and zero-valent iron (ZVI)) are usually chosen to removal As from water (Hao et al. 2018, Adlnasab et al. 2019, Uddin and Jeong 2020).

Magnetite (Fe_3O_4) and hematite (α-Fe_2O_3) are the major derivatives of iron oxide which facilitate the As remediation. These iron oxides have been utilized to remove As from water (Siddiqui et al. 2019). Iron oxide nanoparticles possess attractive properties such as super-paramagnetism at room temperature, which is an efficient and convenient method to separate As-adsorbed particles (Wong et al. 2017). Also, zero valent iron (ZVI) or metallic iron (Fe^0) is a cost-effective agent for removal of inorganic and organic pollutants (Siddiqui et al. 2019). Nano-ZVI can be distributed or dispersed in the subsurface of water which carries the contaminants (Siddiqui et al., 2019). Many studies have suggested that nano-ZVI chemistry allows the safe, effective, and economic reduction of As from water (Tanboonchuy et al. 2011, Li et al. 2014, Adio et al. 2017, Li et al. 2017).

Adsorption of arsenic by various adsorbents is a complex process involving different mechanisms and controlled by different variables. Factors such as solution pH, contact time, nature of adsorbent, initial metal ion concentration, particle size of adsorbent, and presence of competing contaminant ions can influence As removal from water. Optimizing these factors might give excellent outcomes for As treatment (Wong et al. 2017, Uddin and Jeong 2020). Over the years, conventional optimization in which a process parameter is varied while other parameters are kept constant is expensive and time-consuming. Nevertheless, a more robust technique to optimize several process parameters has been provided by Taguchi (Idris et al. 2020, Egbosiuba et al. 2021). Taguchi optimization method is highly effective in optimizing multifactor with a minimum number of experiments, thereby reducing cost and improving quality (Maazinejad et al. 2020, Egbosiuba et al. 2021). Also, the Taguchi optimization method is one such method that has several advantages over the conventional "one-at-a-time" because it provides us with more information from fewer experiment runs (Yadav et al. 2015). Despite the several applications of iron particles in environmental sciences and As adsorption, optimization of the adsorption processes is less known. Also, little information was found about the removal efficiency of iron-based materials with different particle size. Therefore, the objective of this study was to compare the adsorption capacity of iron-based particles and investigate the optimum conditions of some factors such as contact time, initial As concentration, pH and adsorbent dose, type, and size for the maximum adsorption of As from the aqueous solution using the Taguchi method. Furthermore, Langmuir and Freundlich adsorption isotherms were studied to explain the As adsorption mechanism.

MATERIALS AND METHODS

Synthesis of iron oxides and ZVI nanomaterials

All the chemicals used were of analytical grade and obtained from Merck Company. Hematite, magnetite, and ZVI nanomaterials were synthesized using hydrothermal (Trpkov et al. 2018), co-precipitation (Hedayati et al. 2017), and green methods (Wang et al. 2014), respectively. Hematite particles were

synthesized by mixing 0.01 mol/L of $FeCl_2.4H_2O$ and 0.02 mol/L of Fe $(NO_3)_3$ and 10 mL of ammonia solution at room temperature (Trpkov et al. 2018). The mixture was then transferred to a 120 mL galvanized stainless-steel autoclave and reacted at 200 ºC for 2, 4, and 6 hours to control different size of nanoparticles. After the reaction, the autoclave was cooled and the dark precipitates were collected by centrifugation and washed three times with distilled water and ethanol. Finally, the precipitate was dried at 70 ºC for 12 hours. For the synthesis of magnetite particles, 0.01 mol $FeCl_2.4H_2O$ and 0.02 mol $FeCl_3.9H_2O$ were dissolved in 100 mL of water and then a mixture of 10 mL of 25 % ammonia were slowly added to the solution under nitrogen atmosphere. The quality of hematite particles was controlled by adjusting the reaction temperature from 60 to 150 ºC. The final precipitate was centrifuged and washed with distilled water and air dried (Hedayati et al. 2017). To synthesize the ZVI particles, eucalyptus leaves were used. It is probably that the eucalyptus leaf extract is a mixture of various naturally derived compounds with different reducing properties (Wang et al. 2014). Eucalyptus leaves were obtained from a local farm in Rafsanjan, Kerman province, Iran. Deionized (DI) water was used in all experiments. First, leaves were thoroughly washed with distilled water and then dried at room temperature. The plant extract was prepared by adding 15 g of dried leaves in 250 mL of distilled water for 1 hour at 80 ºC. The extract was then filtered in a vacuum and stored at 4 ºC. To prepare the ZVI nanomaterials with different sizes, the eucalyptus extract was stirred with 0 0.1 mol/L Fe $(SO_4).2H_2O$ in a ratio of 1:1, 1:2, and 1:3 at room temperature for 30 min. The precipitates were then collected in a vacuum and washed three times with ethanol. Finally, the ZVI nanomaterials particles were dried under a vacuum for 12 hours at 50 ºC and stored in a nitrogen atmosphere (Wang et al. 2014).

Characterization of iron-based particles

The morphological characteristics of iron-based particles were analyzed by field emission scanning electron microscopy (FESEM, ZEISS, Sigma VP) coupled with an energy dispersive X-ray (EDX). The Powder X-ray diffraction (XRD) data were collected on a Bruker D8 Advance X-ray diffractometer (Cu Ka X-radiation at 40 kV and 40 mA).

Adsorption studies

The As adsorption optimization process was performed using the standard method proposed by Taguchi to achieve maximum adsorption of As ions. The Taguchi method utilizes an orthogonal array (OA) for experimental design and applies the signal-to-noise ratio (S/N) for quality evaluation (Huang et al. 2009, Paul et al. 2014, Zolgharnein and Rastgordani 2018). There are several types of S/N, such as the smaller is better, the larger is better and the nominal is better. In this paper, the larger is better S/N was determined because the purpose of this work was to achieve a high adsorption percentage. Thus, the eq. 1 presented by Taguchi for S/N calculation the larger-the better criteria was:

$$\left(\frac{S}{N}\right) = -10\log\left[\frac{1}{n}\sum_{i=1}^{n}\frac{1}{y_i^2}\right] \quad (1)$$

Where y_i is the experimental response (As adsorption percentage), and **n** is the repetition number of the experiment. The suggested design with 27 experiments conducted for the selected factors with their corresponding levels is presented in **table I**. Six controllable factors were considered to design

TABLE I. CONTROLLABLE FACTORS AND THEIR LEVELS IN THE TAGUCHI METHOD.

Factor	Level		
	1	2	3
(X1) Contact time (h)	0.5	2	4
(X2) pH	6	7	9
(X3) Adsorbent size*	*	**	***
(X4) Adsorbent type	Hematite	Magnetite	ZVI
(X5) Initial As concentration (µg/L)	500	1000	3000
(X6) Adsorbent dose (g)	0.01	0.06	0.1

*: average particle size > 80 nm, ** average particle size 30-80 nm, *** average particle size < 30 nm.

the experiment, including contact time, pH, adsorbent size, adsorbent type, initial concentration, and adsorbent dose, each at three different levels. These factors' levels were selected based on previous works and preliminary experiments.

Table II presents the required experiments to optimize the batch adsorption system designed using the Taguchi method. In each run, the As adsorption capacity by the iron-based particles was investigated using the background electrolyte of 0.01 mol/L $NaNO_3$ at room temperature (25 ºC). For this purpose, 0.05 g of each iron-based particle (with three different sizes and at desired pH values) was added to polyethylene containers containing 10 mL of arsenic solution with an initial concentration of 500-3000 µg/L. Samples were then shaken at the speed of 150 rpm for 24 h. Then the supernatant was separated from the solid by centrifugation at 20 000 g for 20 min. The concentration of As was then analyzed by graphite furnace atomic absorption spectrophotometry (SavantAA, GBC). All experiments were repeated three times.

TABLE II. L27 ORTHOGONAL ARRAY (LEVEL OF SIX DIFFERENT FACTORS; CONTACT TIME (X1), pH (X2), ADSORBENT SIZE (X3), ADSORBENT TYPE (X4), INITIAL ARSENIC CONCENTRATIONS (X5), ADSORBENT DOSE (X6) AND EXPECTED RESULTS.

Run	X1	X2	X3	X4	X5	X6	q_e (µg/g)	S/N ratio
1	1	1	1	1	1	1	71.1	37.04
2	1	1	1	1	2	2	290.45	49.26
3	1	1	1	1	3	3	744	57.43
4	2	1	2	2	1	1	28.5	29.10
5	2	1	2	2	2	2	202.6	46.13
6	2	1	2	2	3	3	736	57.34
7	3	1	3	3	1	1	332.1	50.43
8	3	1	3	3	2	2	1112.5	60.93
9	3	1	3	3	3	3	1365.5	62.71
10	1	2	2	3	1	1	17.9	25.06
11	1	2	2	3	2	2	152	43.64
12	1	2	2	3	3	3	671	56.53
13	2	2	3	1	1	1	61.7	35.81
14	2	2	3	1	2	2	408	52.21
15	2	2	3	2	3	3	1225.5	61.77
16	3	2	1	2	1	1	88.4	38.93
17	3	2	1	2	2	2	323	50.18
18	3	2	1	2	3	3	2616.5	68.35
19	1	3	3	2	1	1	125.8	41.99
20	1	3	3	2	2	2	1073	60.61
21	1	3	3	2	3	3	1548.5	63.80
22	2	3	1	3	1	1	227.3	47.13
23	2	3	1	3	2	2	1080	60.67
24	2	3	1	3	3	3	1660	64.40
25	3	3	2	1	1	1	71.47	37.08
26	3	3	2	1	2	2	1098.5	60.82
27	3	3	2	1	3	3	1195	61.55

Adsorption isotherms of As onto the adsorbents were determined in batch experiments. Ten milliliters of 0.01 mol/L $NaNO_3$ solution with different concentration ranges of As (100-6800 µg/L) were added into centrifuge tubes containing 0.05 g adsorbent. Blank samples (without adsorbent) were also considered for each concentration of As. The pH values of the suspensions were adjusted to 7.0 by adding 100-300 µL of 0.03 mol/L NaOH or HNO_3 solution. The suspensions were shaken for 4 h with a rotary shaker at a speed of 150 rpm. The equilibrium solutions were separated by centrifugation for 20 min at 20 000 g, and As concentration was measured using graphite furnace atomic absorption spectrophotometry (SavantAA, GBC). All experiments were repeated three times. The amount of As adsorbed per unit mass of the adsorbent was evaluated, using the eq. 2:

$$q_e = \frac{(C_i - C_e)}{m} \times V \tag{2}$$

where C_i and C_e are the initial and equilibrium concentrations of As (µg/L) in solutions, respectively. q_e (µg/g) is adsorption capacity, V (L) is the volume of solution, and m (g) is the mass of adsorbent.

The removal percentage of As was calculated for each experiment by eq. 3:

$$Removal\ (\%) = \frac{(c_i - c_e)}{c_i} \times 100 \tag{3}$$

The equilibrium adsorption data were analyzed with the utilization of the Freundlich and Langmuir equilibrium isotherms. Eqs. 4 and 5 represent non-linear form of Freundlich and Langmuir isotherms, respectively (Hamidpour et al. 2018).

$$q_e = \frac{q_{max} b c_e}{1 + b c_e} \tag{4}$$

$$q_e = K_f c_e^{\frac{1}{n}} \tag{5}$$

Where C_e is the equilibrium concentration of the As (µg/L), q_e denotes the amount of the As adsorbed per unit mass of the adsorbent at equilibrium (µg/g), q_{max}(µg/g), and b (L/µg) are the Langmuir constants related to the monolayer uptake capacity and energy of adsorption, respectively (Zhou et al. 2020). The K_f (L/g) and 1/n (-) are the Freundlich constants.

The parameters of adsorption isotherms were determined by the non-linear curve fitting analysis method using the DataFit statistical software.

RESULTS

Characterization

XRD analysis

The characterization by X-ray diffraction (XRD) results are displayed in **figure 1**. The successful synthesis of iron-based nanoparticles was proved by XRD analysis. All diffraction peaks in **figure 1** can be indexed to the hematite and magnetite crystalline phase, which are in accordance with the data reported in the literature (Compeán-Jasso et al. 2008, Cuong et al. 2014). The XRD patterns of the synthesized ZVI nanoparticles had a broad peak, indicating the production of an amorphous structure (Ebrahiminezhad et al. 2017, Kheshtzar et al. 2019). Fabrication of amorphous ZVI was also reported by using leaf extract of different plants and food industry wastes (Wang et al. 2014, Ebrahiminezhad et al. 2017).

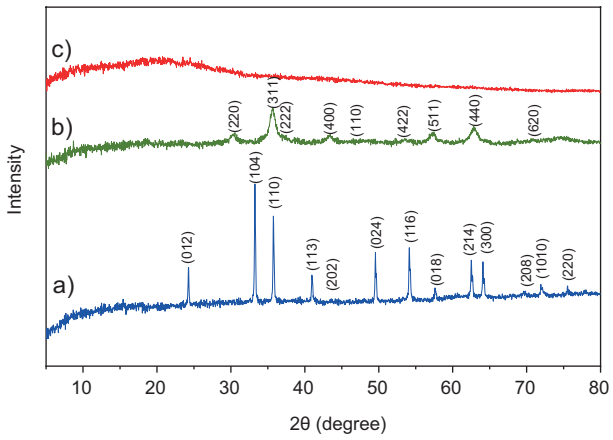

Fig. 1. XRD of iron-based particles; a) Hematite, b) Magnetite, and c) Zero-valent iron.

FESEM analysis

The morphology of the synthesized iron-based nanoparticles was evaluated using FESEM (**Fig. 2**). In **figure 2a**, the well-developed hematite spheres are seen. Some representative images in **figure 2** indicated that the hierarchically assembled hematite sphere was a multi-scale organized nanoarchitecture. Also, the FESEM image in **figure 2b** shows that the prepared magnetite sphere possesses dense nanostructures on its surface, constructing a hierarchical dandelion-like structure. Although it is difficult to identify an individual nanostructure from the FESEM image, it can be found that the synthesized magnetite nanostructures were aligned on the surface of the particles. **Figure 2c** shows a FESEM image of ZVI

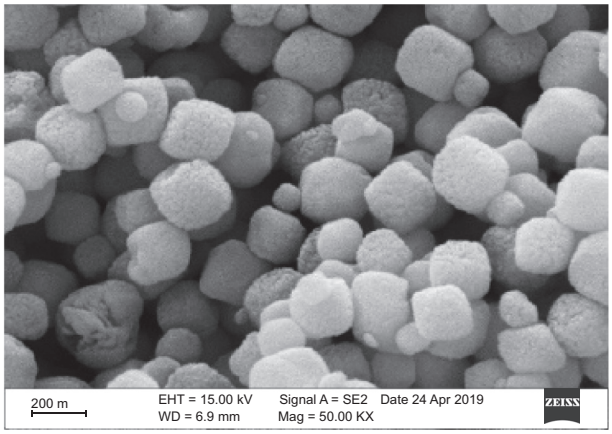

a) Hematite

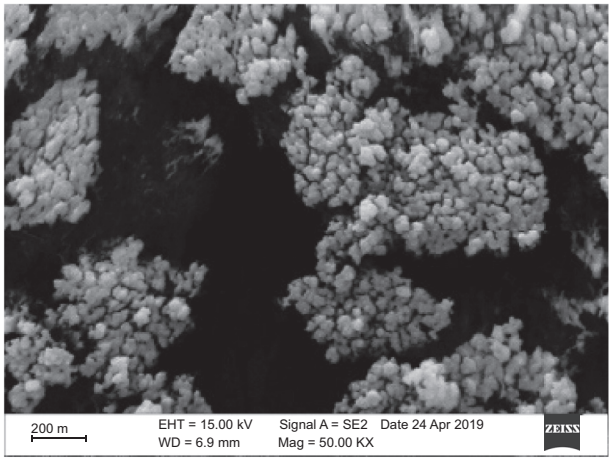

b) Magnetite

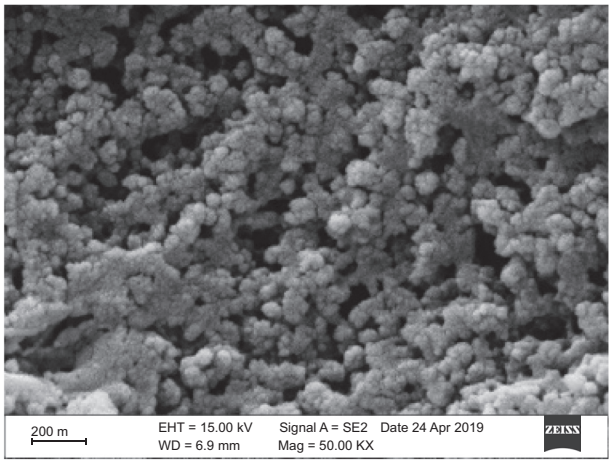

c) Zero-valent iron

Fig. 2. Field emission scanning electron microscopy (FESEM) micrograph of a) Hematite, b) Magnetite, and c) Zero-valent iron particles at 50 KX magnification

nanomaterials. In the FESEM image of ZVI, the formation of some irregular shapes due to aggregation and fusion of the particles was observed.

Taguchi method

Analysis of signal/noise ratio

In this study, six controllable factors were chosen as input variables and each factor was evaluated at three levels according to an L27 orthogonal array designed by the Taguchi method (**Table I**). The adsorption capacity (q_e) of As was chosen as a response in the Taguchi L27 array. Since in the case of As ions adsorption "Larger is better" is the desired case, the optimum level of the controllable factors was the level that corresponds to the highest S/N ratio according to eq. 1. The experimental results for As ions adsorption and the S/N ratio values are reported in **table II**. The objective of applying the Taguchi method is to determine the optimum conditions at which *q*e is maximized (Yadav et al. 2015, Googerdchian et al. 2018).

According to the S/N ratio, the optimum levels of the factors for obtaining the maximum response variable (removal percentage of As) are shown in **figure 3**. It is observed that initial As concentration had a remarkable effect on the adsorption process (**Fig. 3e**). An increase of the As initial concentration accelerates the diffusion of As from the solution onto the adsorbents due to the increasing driving force at higher ion concentration (Hamidpour et al. 2018).

Figure 3b shows the effect of solution pH on As uptake. As expected, an increase in the pH leads to an increase in As removal percentage. In the process of As removal from aqueous solutions, the pH value of the solution is a significant factor since it affects both the As speciation and the surface charge of the adsorbents due to protonating or deprotonating of surfaces of the adsorbents (Bilici-Baskan and Hadimlioglu 2020). The species of As are negatively charged where the solution pH value is more than 2.2. Arsenic species were attracted to the

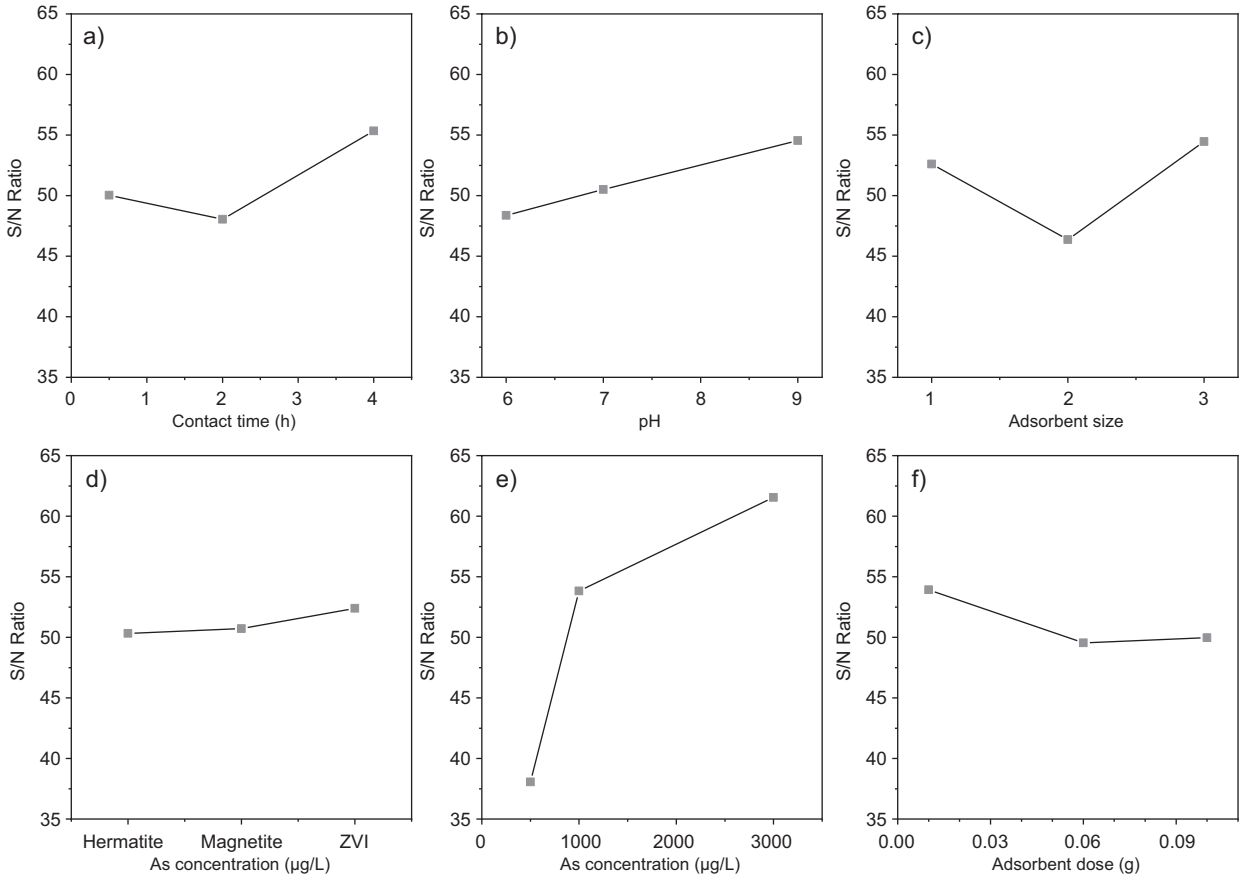

Fig. 3. The main effect of each factor by signal-to-noise (S/N) ratio for different factors: a) Contact time, b) pH, c) Adsorbent size, d) Adsorbent type, e) Initial As concentration and f) Adsorbent dose. Signal-to-noise ratio: The larger-The better.

positively charged surfaces of iron-based adsorbents by the effect of electrostatic forces. Bilici-Baskan and Hadimlioglu (2020) reported similar findings for the adsorption of As onto graphene oxide-iron modified clinoptilolite composites. According to **figure 3**, the optimum condition was found to be adsorbent dose = 0.01 g/L, initial As concentration = 3000 µg/L, pH = 9, contact time = 4 h, adsorbent type = ZVI, and adsorbent size < 30 nm in the studied range for different parameters.

Figure 4 graphically depicts the contribution of each parameter to As adsorption. The percent contributions (ρ) of initial As concentration, adsorbent size, contact time, pH adsorbent dose, and adsorbent type, were 74.5 %, 9.4 %, 7.4 %, 5.1 %, 3 % and 0.06 %, respectively. The initial As concentration had the greatest ρ. However, the adsorbent type had the lowest ρ.

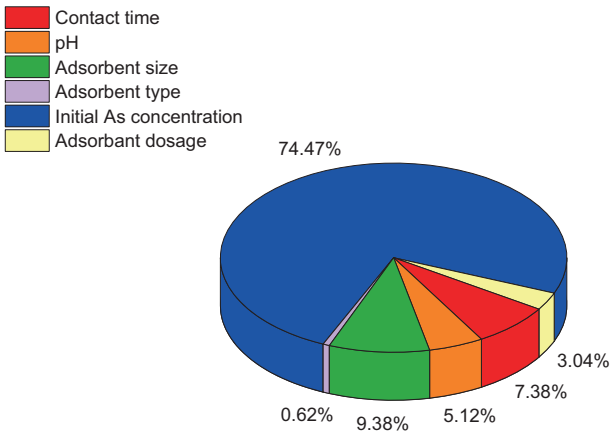

Fig. 4. Contribution percentage (ρ) of factors for adsorption capacity of iron particles.

Response tables related to the calculated S/N ratios are shown in **table III**. Also, the significance of controllable factors might be determined by the rank of S/N ratio given in **table III** (the symbol "Δ" shows the difference between the maximum and minimum S/N ratios). The more significant factor shows a larger range and should be utilized first (Zolgharnein and Rastgordani 2018). It was evident from the ranks obtained for each factor that initial As concentrations and size of adsorbent were the most influential factors (rank 1 and 2) for the responses of qe. The rank was initial As concentration (23.48) > size of adsorbent (8.11) > contact time (7.29) > pH (6.18) > adsorbent dosage (4.38) > type of adsorbent (2.06) in descending order (**Table III**).

Adsorption isotherms

Adsorption isotherms exhibit As distribution between the adsorbent and the bulk solution at equilibrium conditions. The two well-known isotherm equations (Langmuir and Freundlich) were employed for explaining and modeling the experimental data in the systems. The results and their corresponding plots are shown in **table IV** and **figure 5**, respectively. The results of As adsorption was found to fit well with the Freundlich isotherm model due to the larger values of coefficient of determination (R^2) and lower error values of SSE (Zolgharnein and Rastgordani 2018) and adsorption constants evaluated from the isotherms are listed in **table IV**. It follows, therefore, that the adsorption is not limited to a monolayer and that As molecules migrate to heterogeneous surfaces on the iron-based particles following the Freundlich isotherm theory. The Freundlich model describes the multilayer adsorption on heterogeneous adsorbent surfaces with non-identical sites (Adlnasab et al. 2019). The values of n between 1 and 10 (i.e., 1/n less than 1) imply favorable adsorption, and the value of 1/n between 0 and 1 shows the degree of non-linearity between solution concentration and adsorption. If the value of 1/n equals 1, the adsorption is linear. A higher value of Kf reveals a higher adsorption capacity than a lower value (Maji et al. 2018).

The investigated adsorption conditions and adsorption capacities in the present study were compared with the previous studies over the literature as presented in **table V**. The values are reported in

TABLE III. RESPONSE TABLE FOR SIGNAL TO NOISE RATIOS (S/N); LARGER IS BETTER.

Level	Factors					
	Contact time	pH	Adsorbent size	Adsorbent type	Initial As concentration	Adsorbent dose
1	50.04	48.37	52.6	50.33	38.06	53.92
2	48.05	50.51	46.36	50.72	53.83	49.54
3	55.34	54.55	54.47	52.39	61.54	49.97
Δmax-min	7.29	6.18	8.11	2.06	23.48	4.38
Rank	3	4	2	6	1	5

TABLE IV. PARAMETERS OF THE ISOTHERM MODELS.

Iron particle	Langmuir isotherm model		
	b (L/μg)	q_m (μg/g)	R^2
Magnetite1	0.0010	1199.5	0.85
Magnetite2	0.0009	1990	0.95
Magnetite3	0.0055	2000	0.97
NZVI1	0.027	1490	0.50
NZVI2	0.0230	1900	0.84
NZVI3	0.0050	1989	0.84
Hematite1	0.0020	1990	0.87
Hematite2	0.0029	2398	0.80
Hematite3	0.0045	1499	0.66
Iron particle	Freundlich isotherm model		
	K_f (L/g)	n	R^2
Magnetite1	2.86×10^{-6}	0.371	0.980
Magnetite2	0.273	0.826	0.996
Magnetite3	11.276	1.168	0.974
Zero-valent iron1 (ZVI1)	2.02×10^{-9}	0.141	0.887
Zero-valent iron2 (ZVI2)	8.941	0.754	0.889
Zero-valent iron3 (ZVI3)	0.811	0.715	0.964
Hematite1	0.018	0.568	0.993
Hematite2	15.618	1.329	0.771
Hematite3	0.051	0.560	0.759

the form of monolayer adsorption capacity. High adsorption capacities of some adsorbents may be due to the high As concentrations taken in performing the batch experiments. The experimental data of the present study show that iron-based adsorbents exhibited a reasonable adsorption capacity for As and, therefore, may help remove As from polluted waters. In general, iron-based adsorbents have a high affinity for As species. The formation of inner-sphere surface complexes is the primary mechanism for the strong interactions between As species and the functional groups on the adsorbent surfaces. (Bilici-Baskan and Hadimlioglu 2020, Feng et al. 2012).

CONCLUSION

This study evaluated the feasibility of iron-based adsorbents (hematite, magnetite, and ZVI) for As adsorption using the Taguchi method to determine the optimum removal condition through 27 trials. The optimum condition was found to be adsorbent dose = 0.01 g/L, initial As concentration = 3000 μg/L,

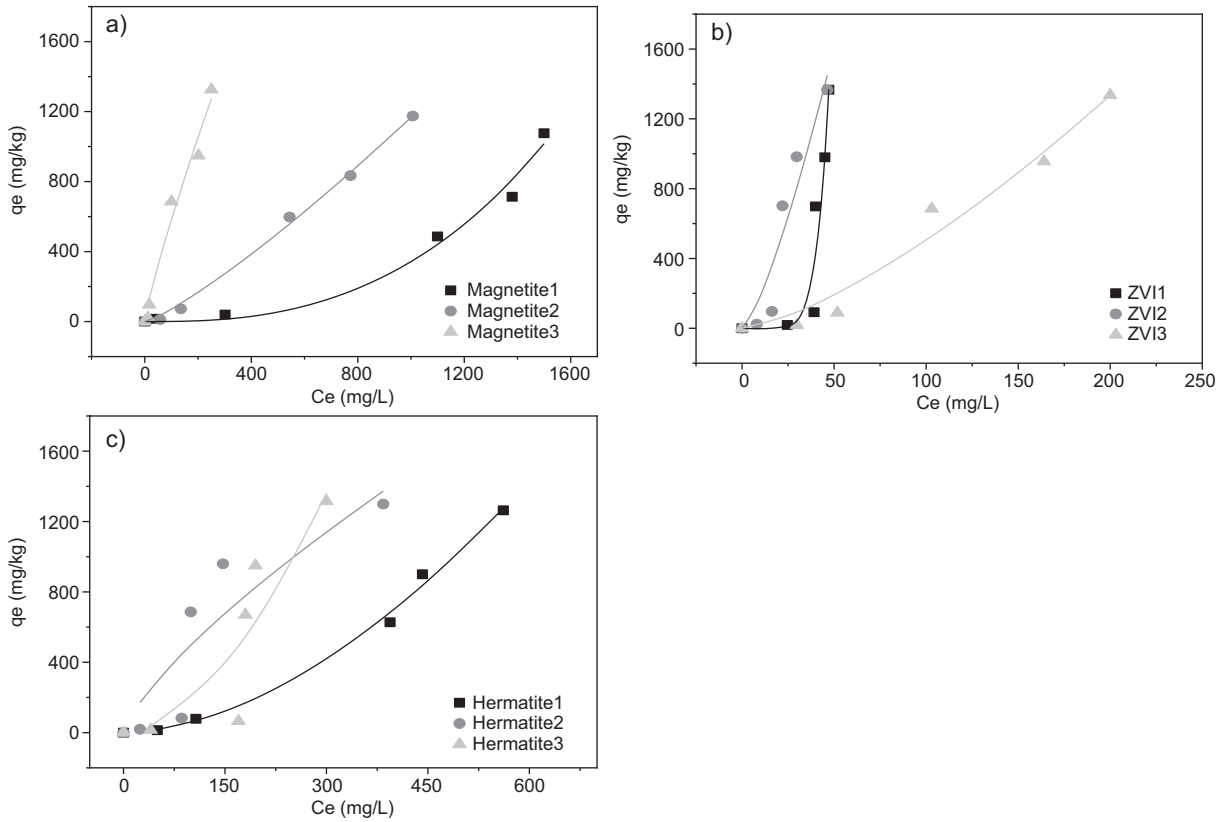

Fig. 5. Adsorption isotherm of As onto a) Hematite b) Magnetite, and c) Zero-valent iron (ZVI).

TABLE V. ADSORPTION CAPACITIES OF DIFFERENT IRON COMPOUNDS FOR ARSENIC.

Adsorbents	pH	Initial concentration (mg/L)	Adsorption capacity (mg/g)	References
α-Fe_2O_3	3-10	1	0.2	Tang et al. 2011
Fe_3O_4 nanoparticles	5	70	16.56	Feng et al. 2012
Zero-valent iron	7	0.2	1.8-2	Biterna et al. 2010
Zero-valent iron	7	_	3.5	Ye et al. 2017
Zero-valent iron	6	2-100	1.7	Wu et al. 2017
Magnetite	6-9	0.1-6.8	2.0	This study
Hematite	6-9	0.1-6.8	2.4	This study
Zero-valent iron	6-9	0.1-6.8	1.9	This study

pH = 9, contact time = 4 h, adsorbent type = ZVI, and adsorbent size < 30 nm in the studied range for different parameters. It is also concluded that the initial As concentration is the most critical parameter in the adsorption process. The As adsorption on the adsorbents conforms well to the Freundlich isotherm compared to the Langmuir model. This research revealed that iron-based adsorbents used in this study show high adsorption behavior for removing arsenic from water.

REFERENCES

Adio S.O., Omar M.H., Asif M. and Saleh T.A. (2017). Arsenic and selenium removal from water using biosynthesized nanoscale zero-valent iron: A factorial design analysis. Process Safety and Environmental Protection 107, 518-527. https://doi.org/10.1016/j.psep.2017.03.004

Adlnasab L., Shekari N. and Maghsodi A. (2019). Optimization of arsenic removal with Fe_3O_4@Al_2O_3@Zn-Fe LDH as a new magnetic nano adsorbent using Box-Behnken design. Environmental Chemical Engineering 7 (2), 102974. https://doi.org/10.1016/j.jece.2019.102974

Ajiboye T.O., Oyewo O.A. and Onwudiwe D.C. (2021). Simultaneous removal of organics and heavy metals from industrial wastewater: A review. Chemosphere 262, 128379. https://doi.org/10.1016/j.chemosphere.2020.128379

Bilici-Baskan M. and Hadimlioglu S. (2021). Removal of arsenate using graphene oxide-iron modified clinoptilolite-based composites: adsorption kinetic and column study. Journal of Analytical Science and Technology 12, 22. https://doi.org/10.1186/s40543-021-00274-6

Biterna M., Antonoglou L., Lazou E. and Voutsa D. (2010). Arsenite removal from waters by zero valent iron: Batch and column tests. Chemosphere 78, 7-12. https://doi.org/10.1016/j.chemosphere.2009.10.007

Cao Q., Chen C., Li K., Sun T., Shen Z. and Jia J. (2021). Arsenic(V) removal behavior of schwertmannite synthesized by $KMnO_4$ rapid oxidation with high adsorption capacity and Fe utilization. Chemosphere 264, 128398. https://doi.org/10.1016/j.chemosphere.2020.128398

Chaudhry S.A., Zaidi Z. and Siddiqui S.I. (2017). Isotherm, kinetic and thermodynamics of arsenic adsorption onto iron-zirconium binary oxide-coated sand (IZBOCS): Modelling and process optimization. Journal of Molecular Liquids 229, 230-240. https://doi.org/10.1016/j.molliq.2016.12.048

Compeán-Jasso M.E., Ruiz F., Martínez J.R. Herrera-Gómez A. (2008). Magnetic properties of magnetite nanoparticles synthesized by forced hydrolysis. Materials Letters 62, 4248-4250. https://doi.org/10.1016/j.matlet.2008.06.053

Cuong N.D., Hoa N.D., Hoa T.T., Khieu D.Q., Quang D.T., Quang V. Van and Hieu N. Van (2014). Nanoporous hematite nanoparticles: Synthesis and applications for benzylation of benzene and aromatic compounds. Journal of Alloys and Compounds 582, 83-87. https://doi.org/10.1016/j.jallcom.2013.08.057

Ebrahiminezhad A., Zare-Hoseinabadi A., Berenjian A. and Ghasemi Y. (2017). Green synthesis and characterization of zero-valent iron nanoparticles using stinging nettle (*Urtica dioica*) leaf extract. Green Processing and Synthesis 6, 469–475. https://doi.org/10.1515/gps-2016-0133

Egbosiuba T.C., Abdulkareem A.S., Tijani J.O., Ani J.I., Krikstolaityte V., Srinivasan M., Veksha A. and Lisak G. (2021). Taguchi optimization design of diameter-controlled synthesis of multi walled carbon nanotubes for the adsorption of Pb(II) and Ni(II) from chemical industry wastewater. Chemosphere 266, 128937. https://doi.org/10.1016/j.chemosphere.2020.128937

Feng L., Cao M., Ma X., Zhu Y. and Hu C. (2012). Superparamagnetic high-surface-area Fe_3O_4 nanoparticles as adsorbents for arsenic removal. Journal of Hazardous Materials 217-218, 439–446. https://doi.org/10.1016/j.jhazmat.2012.03.073

Googerdchian F., Moheb A., Emadi R. and Asgari M. (2018). Optimization of Pb(II) ions adsorption on nanohydroxyapatite adsorbents by applying Taguchi method. Journal of Hazardous Materials 349, 186-194. https://doi.org/10.1016/j.jhazmat.2018.01.056

Hamidpour M., Hosseini N., Mozafari V. and Heshmati-Rafsanjani M. 2018. Removal of Cd(II) and Pb(II) from aqueous solutions by pistachio hull waste. Revista Internacional de Contaminación Ambiental 34 (2), 307-316. https://doi.org/10.20937/rica.2018.34.02.11

Hao L., Liu M., Wang N. and Li G. (2018). A critical review on arsenic removal from water using iron-based adsorbents. RSC Advances 8, 39545–39560. https://doi.org/10.1039/c8ra08512a

Hedayati K., Goodarzi M. and Ghanbari D. (2017). Hydrothermal synthesis of Fe_3O_4 nanoparticles and flame resistance magnetic poly styrene nanocomposite. Journal of Nanostructure 7, 32-39. https://doi.org/10.22052/jns.2017.01.004

Huang H., Cheng G., Chen L., Zhu X. and Xu H. (2009). Lead (II) removal from aqueous solution by spent *Agaricus bisporus*: determination of optimum process condition using Taguchi method. Water, Air, and Soil Pollution 203, 53-63. https://doi.org/10.1007/s11270-009-9991-1

Idris F.N., Nadzir M.M. and Abd Shukor S.R. (2020). Optimization of solvent-free microwave extraction of *Centella asiatica* using Taguchi method. Journal of Environmental Chemical Engineering 8, 103766. https://doi.org/10.1016/j.jece.2020.103766

Kheshtzar R., Berenjian A., Taghizadeh S.M., Ghasemi Y., Asad A.G. and Ebrahiminezhad A. (2019). Optimization of reaction parameters for the green synthesis of zero valent iron nanoparticles using pine tree needles. Green Processing and Synthesis 8, 846-855. https://doi.org/10.1515/gps-2019-0055

Li S., Wang W., Liang F. and Zhang W.X. (2017). Heavy metal removal using nanoscale zero-valent iron (nZVI): Theory and application. Journal of Hazardous Materials 322, 163-171. https://doi.org/10.1016/j.jhazmat.2016.01.032

Li S., Wang W., Liu Y. and Zhang W. (2014). Zero-valent iron nanoparticles (nZVI) for the treatment of smelting wastewater: A pilot-scale demonstration. Chemical Engineering Journal 254, 115-123. https://doi.org/10.1016/j.cej.2014.05.111

Maazinejad B., Mohammadnia O., Ali G.A.M., Makhlouf, A.S.H., Nadagouda M.N., Sillanpää M., Asiri A.M., Agarwal S., Gupta V.K. and Sadegh H. (2020). Taguchi L9 (3^4) orthogonal array study based on methylene blue removal by single-walled carbon nanotubes-amine: Adsorption optimization using the experimental design method, kinetics, equilibrium and thermodynamics. Journal of Molecular Liquids 298, 112001. https://doi.org/10.1016/j.molliq.2019.112001

Maji S., Ghosh A., Gupta K., Ghosh A., Ghorai U., Santra A., Sasikumar P. and Ghosh U.C. (2018). Efficiency evaluation of arsenic(III) adsorption of novel graphene oxide@iron-aluminium oxide composite for the contaminated water purification. Separation and Purification Technology 197, 388-400. https://doi.org/10.1016/j.seppur.2018.01.021

Paul M.L., Samuel J., Chandrasekaran N. and Mukherjee A. (2014). Preparation and characterization of layer-by-layer coated nano metal oxides-polymer composite film using Taguchi design method for Cr(VI) removal. Journal of Environmental Chemical Engineering 2, 19 37-1946. https://doi.org/10.1016/j.jece.2014.08.018

Siddiqui S.I., Naushad M. and Chaudhry S.A. (2019). Promising prospects of nanomaterials for arsenic water remediation: a comprehensive review. Process Safety and Environmental Protection 126, 60-97. https://doi.org/10.1016/j.psep.2019.03.037

Tanboonchuy V., Hsu J.C., Grisdanurak N. and Liao C.H. (2011). Gas-bubbled nano zero-valent iron process for high concentration arsenate removal. Journal of Hazardous Materials 186, 2123-2128. https://doi.org/10.1016/j.jhazmat.2010.12.125

Tang W., Li Q., Gao S. and Shang J.K. (2011). Arsenic (III,V) removal from aqueous solution by ultrafine α-Fe_2O_3 nanoparticles synthesized from solvent thermal method. Journal of Hazardous Materials 192, 131-138. https://doi.org/10.1016/j.jhazmat.2011.04.111

Trpkov D., Panjan M., Kopanja L. and Tadić M. (2018). Hydrothermal synthesis, morphology, magnetic properties and self-assembly of hierarchical α-Fe_2O_3 (hematite) mushroom-, cube- and sphere-like superstructures. Applied Surface Science 457, 427-438. https://doi.org/10.1016/j.apsusc.2018.06.224

Uddin M.J. and Jeong Y.K. (2020). Review: Efficiently performing periodic elements with modern adsorption technologies for arsenic removal. Environmental Science and Pollution Research 27, 39888-39912. https://doi.org/10.1007/s11356-020-10323-z

Wang T., Jin X., Chen Z., Megharaj M. and Naidu R. (2014). Green synthesis of Fe nanoparticles using eucalyptus leaf extracts for treatment of eutrophic wastewater. Science of the Total Environment 466-467, 210–213. https://doi.org/10.1016/j.scitotenv.2013.07.022

Wong W., Wong H.Y., Badruzzaman A.B.M., Goh H.H. and Zaman M. (2017). Recent advances in exploitation of nanomaterial for arsenic removal from water: a review. Nanotechnology 28 (4), 042001. https://doi.org/10.1088/1361-6528/28/4/042001

Wu C., Tu J., Liu W., Zhang J., Chu S., Lu G., Lin Z. and Dang Z. (2017). The double influence mechanism of pH on arsenic removal by nano zero valent iron: Electrostatic interactions and the corrosion of Fe. Environmental Science: Nano 4, 1544-1552. https://doi.org/10.1039/c7en00240H

Yadav K.K., Dasgupta K., Singh D.K., Varshney L. and Singh H. (2015). Dysprosium sorption by polymeric composite bead: Robust parametric optimization using Taguchi method. Journal of Chromatography A 1384, 37-43. https://doi.org/10.1016/j.chroma.2015.01.061

Ye L., Liu W., Shi Q. and Jing C. (2017). Arsenic mobilization in spent nZVI waste residue: Effect of *Pantoea* sp. IMH. Environmental Pollution 230, 1081-1089. https://doi.org/10.1016/j.envpol.2017.07.074

Zhou J., Zhou X., Yang K., Cao Z., Wang Z., Zhou C., Baig S.A. and Xu X. (2020). Adsorption behavior and mechanism of arsenic on mesoporous silica modified by iron-manganese binary oxide (FeMnOx/SBA-15) from aqueous systems. Journal of Hazardous Materials 384, 121229. https://doi.org/10.1016/j.jhazmat.2019.121229

Zhu H., Jia Y., Wu X. and Wang H. (2009). Removal of arsenic from water by supported nano zero-valent iron on activated carbon. Journal of Hazardous Materials 172, 1591-1596. https://doi.org/10.1016/j.jhazmat.2009.08.031

Zolgharnein J. and Rastgordani M. (2018). Optimization of simultaneous removal of binary mixture of indigo carmine and methyl orange dyes by cobalt hydroxide nano-particles through Taguchi method. Journal of Molecular Liquids 262, 405-414. https://doi.org/10.1016/j.molliq.2018.04.038